

Laplacian-dependent models of the kinetic energy density: Applications in subsystem density functional theory with meta-generalized gradient approximation functionals

Szymon Śmiga,^{1,2,3} Eduardo Fabiano,^{4,3} Lucian A. Constantin,³ and Fabio Della Sala^{4,3}

¹*Istituto Nanoscienze-CNR, Italy*

²*Institute of Physics, Faculty of Physics, Astronomy and Informatics,
Nicolaus Copernicus University, Grudziadzka 5, 87-100 Torun, Poland*

³*Center for Biomolecular Nanotechnologies @UNILE,*

Istituto Italiano di Tecnologia (IIT), Via Barsanti, 73010 Arnesano (LE), Italy

⁴*Institute for Microelectronics and Microsystems (CNR-IMM),
Via Monteroni, Campus Unisalento, 73100 Lecce, Italy*

The development of semilocal models for the kinetic energy density (KED) is an important topic in density functional theory (DFT). This is especially true for subsystem DFT, where these models are necessary to construct the required non-additive embedding contributions. In particular, these models can also be efficiently employed to replace the exact KED in meta-Generalized Gradient Approximation (meta-GGA) exchange-correlation functionals allowing to extend the subsystem DFT applicability to the meta-GGA level of theory.

Here, we present a two-dimensional scan of semilocal KED models as linear functionals of the reduced gradient and of the reduced Laplacian, for atoms and weakly-bound molecular systems. We find that several models can perform well but in any case the Laplacian contribution is extremely important to model the local features of the KED. Indeed a simple model constructed as the sum of Thomas-Fermi KED and 1/6 of the Laplacian of the density yields the best accuracy for atoms and weakly-bound molecular systems. These KED models are tested within subsystem DFT with various meta-GGA exchange-correlation functionals for non-bonded systems, showing a good accuracy of the method.

I. INTRODUCTION

Advances in Kohn-Sham density functional theory [1, 2] are strictly related to the availability of accurate and efficient approximations for the exchange-correlation (XC) functional. Over the years, many XC functionals have been proposed [3, 4]. The simplest ones, namely the local density approximation (LDA) [1] and the generalized gradient approximations [5] (GGAs), display an explicit dependence on the electron density (and its gradient). Thus, they are practical tools within the KS scheme. More advanced methods are developed introducing additional input ingredients, that are not explicit functionals of the density. The most notable examples in this context are the hybrid [6, 7] and the meta-GGA [8, 9] XC functionals. The former include a fraction of Hartree-Fock exchange energy and are thus true non-local approaches. The meta-GGA functionals instead have the general form

$$E_{xc} = \int e_{xc}(\rho(\mathbf{r}), \nabla\rho(\mathbf{r}), \tau^{\text{KS}}(\mathbf{r})) d^3\mathbf{r}, \quad (1)$$

where

$$\tau^{\text{KS}}(\mathbf{r}) = \frac{1}{2} \sum_i^{\text{occ.}} |\nabla\phi_i(\mathbf{r})|^2 \quad (2)$$

is the positive defined kinetic energy density (KED) (with ϕ_i being the occupied KS orbitals). This ingredient, which characterizes the meta-GGA level of theory, allows the functionals to distinguish different density regions and to achieve high accuracy for a broad range of

systems and properties [8–30]. For these reasons meta-GGA XC functionals are gaining increasing popularity [8, 10–12, 14, 15, 17–21, 27, 29–33]. For a recent Review of meta-GGAs functionals, see Ref. 9.

The positive defined kinetic energy density is a semilocal quantity which is much easier to compute and manage than a fully non-local one such as the exact exchange energy, but it is not an explicit functional of the electron density. Thus, meta-GGA functionals cannot be straightforwardly used in the KS scheme [34–36]. Instead, they are usually implemented in the generalized KS (GKS) framework [37]. This allows to exploit in the best way the semilocal nature of the functional and obtain a favorable computational cost. However, it may pose some difficulties since, in contrast to the KS one, the GKS XC potential is not local [9, 36].

One relevant case where the non-local nature of the potential is particularly troublesome is the subsystem formulation of DFT [38–40], where the nearsightedness principle [41] is employed to partition a complex systems into simpler and smaller subsystems whose interaction is described by embedding potentials. In fact, within subsystem DFT the total ground-state electron density ρ of a given system can be written as

$$\rho(\mathbf{r}) = \sum_{I=1}^M \rho_I(\mathbf{r}) \quad ; \quad \rho_I(\mathbf{r}) = \sum_{i=1}^{N_I} |\phi_i^I(\mathbf{r})|^2, \quad (3)$$

where M is the number of subsystems, N_I is the number of occupied KS orbitals in the I -th subsystem and ϕ_i^I are the KS orbitals of the I -th subsystem, which are obtained

by solving the coupled equations [42, 43]

$$\left[-\frac{1}{2}\nabla^2 + v_s^I(\mathbf{r}) + v_{emb}^I(\mathbf{r}) \right] \phi_i^I(\mathbf{r}) = \epsilon_i^I \phi_i^I(\mathbf{r}). \quad (4)$$

Here v_s^I is the ordinary KS potential relative to subsystem I , whereas

$$v_{emb}^I = \sum_{J \neq I} v_H^J + \frac{\delta T_s^{nadd}}{\delta \rho_I} + \frac{\delta E_{xc}^{nadd}}{\delta \rho_I} \quad (5)$$

is the embedding potential which takes into account the presence of the other subsystems. Equation (5) includes the classical Coulomb potential v_H (electron-nuclei and electron-electron terms) of all the other subsystems. Moreover, it contains the functional derivatives of the non-additive kinetic and XC functionals

$$T_s^{nadd} = T_s \left[\sum_{I=1}^M \rho_I \right] - \sum_{I=1}^M T_s [\rho_I] \quad (6)$$

$$E_{xc}^{nadd} = E_{xc} \left[\sum_{I=1}^M \rho_I \right] - \sum_{I=1}^M E_{xc} [\rho_I]. \quad (7)$$

The non-additive terms of Eqs. (6) and (7) as well as the related functional derivatives cannot be calculated in a direct manner for functionals whose dependence on the density is not known explicitly. This is always the case for kinetic energy, which therefore requires an appropriate semilocal approximation [44–51]. No problem arises instead for LDA or GGA XC functionals. To go beyond the GGA level of theory, however, the standard subsystem DFT formalism based on the KS scheme cannot be easily applied.

Recently, several advances of subsystem DFT have been proposed such as the use of subsystems' fractional occupations [52], the use of orbital-dependent functionals [53], and the embedding of wave-functions in DFT [54, 55]. Moreover, particularly interesting for the present work are an extension to the GKS framework [56] and applications of subsystem DFT calculations using meta-GGA XC functionals [57, 58]. In Ref. 57, we presented a formal approach for subsystem DFT with meta-GGAs: the operational equations are analogous to Eq. (4) but v_s is replaced by the GKS potential of the subsystem while the XC embedding contribution [Eq. (7) and the related derivative] is approximated by a proper semilocal expression. This is obtained by substituting, in the meta-GGA XC functional [Eq. (1)], the orbital-dependent KED τ^{KS} with an approximated semilocal model τ . This computational approach has proven to be remarkably accurate, in spite of the well known difficulty of describing the kinetic energy with semilocal approximations and the fact that the XC functional depends non-linearly on the KED. The reason may be traced back to the fact that in non-additive contributions a prominent role is played by valence regions, whereas the more complicated core contributions to the kinetic energy

are not much relevant. Nevertheless, in previous studies only one meta-GGA XC functional was considered [the Tao-Perdew-Staroverov-Scuseria [8] (TPSS) one] together with two simple models for the kinetic energy density. Thus, a deep understanding of the methodology is still lacking.

In this paper we aim at improving this work. Therefore, in Section II we introduce a whole family of semilocal KED models and in Section IV we test them on different properties and systems, including subsystem DFT calculations using different meta-GGA XC functionals. In this way, we can obtain not only a full assessment of the method and of the various KED models but also a more complete understanding of the basic features that are required to construct successful semilocal KED models. Note that we restrict our study to quite simple KED models, displaying a simple dependence on the gradient and a linear one on the Laplacian of the density. This choice allows to obtain reasonably accurate results avoiding, at the same time, an excessive complexity in the models that would prevent the possibility of a detailed analysis and of a quite complete understanding of the underlying physics. Of course, in search of very accurate and realistic KED models one is required, in general, to go beyond simple functional forms as those considered here. However, this increases significantly the complexity of the problem also because the exploration of the corresponding huge fitting space calls for the use of advanced computational techniques (e.g. machine learning). Hence, we leave this task for future work.

II. SEMILOCAL KED MODELS AND METHODOLOGY

Most of semilocal models for τ^{KS} can be written as

$$\tau = \tau^{\text{TF}} (F(s) + bq) , \quad (8)$$

where $\tau^{\text{TF}} = (3/10)(3\pi^2)^{2/3}\rho^{5/3}$ is the Thomas-Fermi (TF) KED [59–61], $s = |\nabla\rho|/[2(3\pi^2)^{1/3}\rho^{4/3}]$ is the reduced gradient, $q = \nabla^2\rho/[4(3\pi^2)^{2/3}\rho^{5/3}]$ is the reduced Laplacian, $F(s)$ is a GGA enhancement factor (i.e. a function of s), and b is a coefficient. Functionals with the general form in Eq. (8) are named Laplacian-Level meta-GGA (LLMGGA) kinetic energy functionals. If $b = 0$, instead, we have simple GGA kinetic energy functionals.

Among the KED approximations based on Eq. (8), we mention some of particular relevance for the present work:

- The simple TF plus von Weizsäcker approximation (TFW) obtained setting $b = 0$ and $F(s) = 1 + F^{\text{W}}(s)$ with $F^{\text{W}} = (5/3)s^2$, so that $\tau^{\text{W}} = \tau^{\text{TF}} F^{\text{W}}(s)$ is the von Weizsäcker KED [62]. The TFW (GGA) model describes correctly the density-tail asymptotic region in different applications [63]. However, it does not yield in general a very accurate KED [57].

- The second-order gradient expansion (GE2) [64, 65], with $F(s) = F^{\text{GE2}}(s) = 1 + \mu^{\text{GE2}}s^2$, $\mu^{\text{GE2}} = 5/27$ and $b = 20/9$. The GE2 (LLMGGA) describes correctly the slowly-varying density limit.
- The Yang's general formula, obtained from the one-body Green's function in the mean-path approximation considering the Feynman path-integral approach [66]. This has

$$F(s) = F^{\text{Y}}(s) = 1 + \frac{5 - 3b}{9}s^2, \quad (9)$$

where b is the coefficient in Eq. (8). The Yang's LLMGGA model describes accurately the KED of atoms and molecules [67], in particular when $b = 10/9$, which corresponds to $F^{\text{Y}}(s) = F^{\text{GE2}}(s)$.

- The modified GE2 (MGE2) [68] approximation, with $F(s) = F^{\text{MGE2}}(s) = 1 + \mu^{\text{MGE2}}s^2$, $\mu^{\text{MGE2}} = 0.2389$, and $b = 20/9$. The MGE2 (LLMGGA) describes accurately large neutral atoms.
- The APBEK and revAPBEK GGA functionals [47, 48] with $b = 0$ and enhancement factor

$$F^{\text{[rev]APBEK}}(s) = 1 + \left(\frac{1}{\kappa} + \frac{1}{\mu^{\text{MGE2}}s^2} \right)^{-1}, \quad (10)$$

where $\kappa = 0.804$ for APBEK and $\kappa = 1.245$ for revAPBEK. These functionals, in particular revAPBEK, give very accurate non-additive kinetic embedding energies for non-covalently interacting systems [47, 48].

- The τ^L LLMGGA model, having $F(s) = F^{\text{revAPBEK}}(s)$ and $b = 20/9$. This is an extension of the revAPBEK functional, designed to yield the same kinetic energy but a better description of the KED. Indeed, it has been shown to perform well, in subsystem DFT calculations, when it is used to replace τ^{KS} inside a TPSS meta-GGA XC functional [57].

Note that, the Laplacian term in Eq. (8) gives no contribution to the total kinetic energy (for finite systems) nor to the kinetic potential; see appendix A. Thus, it is often omitted in many applications. However, in Refs. 57, 67, 69 it has been shown that the Laplacian term is a very important quantity to describe accurately the spatial dependence of the KED. Nevertheless, because of the presence of this term, most of the models based on Eq. (8) violate one or both of the following exact conditions:

$$\tau^{\text{KS}} \geq 0 \quad (11)$$

$$\tau^{\text{KS}} \geq \tau^{\text{W}}. \quad (12)$$

In fact, as q can be negative in some regions of space, e.g. near the nucleus, then Eq. (11) is easily violated if $b \neq 0$. Instead, the condition in Eq. (12) is harder to satisfy and it is actually respected only by few accurate

functionals [70–73] and by the simple TFW approximation. To avoid this drawback, models based on Eq. (8) can be *regularized* forcing τ to recover τ^{W} near the nucleus [67, 70] (see also Eqs. (19) and (20) later on). In this way, however, the Laplacian term will not integrate to zero, thus the regularization will change the kinetic energy and its functional derivative.

To assess the performance of these models and especially to understand the role of the gradient and Laplacian contributions therein, in this work we consider the general ansatz

$$\tau(a, b) = \tau^{\text{TF}} (1 + as^2 + bq), \quad (13)$$

where a and b are parameters. Equation (13) provides a quite flexible expression which recovers most of the aforementioned KED models. On the other hand, Eq. (13) does not include high-order terms in s , such as the one in Eq. (10). Nevertheless, typical meta-GGA exchange functionals, i.e. TPSS, show a significant dependence on the KED only for small values of s , see Ref. [8]. Thus, the KED needs to be well approximated only in slowly-varying density region.

We perform a full two-dimensional scan of the parameters a and b in Eq. (13) in order to study the possible best performance of the ansatz and understand the role of the different contributions depending on s^2 and q . To this purpose, we consider, for each system, the following error indicators (functions of a and b)

$$\delta_z(a, b) = \frac{1}{N} \int \rho(\mathbf{r}) |z^{\text{KS}} - z(a, b)| d^3\mathbf{r}, \quad (14)$$

$$\delta_\alpha(a, b) = \frac{1}{N} \int \rho(\mathbf{r}) |\alpha^{\text{KS}} - \alpha(a, b)| d^3\mathbf{r}, \quad (15)$$

$$\delta_x(a, b) = \frac{1}{N} \int \rho(\mathbf{r}) |F_x(s, z^{\text{KS}}, \alpha^{\text{KS}}) - F_x(s, z(a, b), \alpha(a, b))| d^3\mathbf{r}, \quad (16)$$

where N is the number of electrons of the system, F_x denotes the TPSS exchange enhancement factor [8], and

$$z^{\text{KS}} = \tau^{\text{W}}/\tau^{\text{KS}}, \quad (17)$$

$$\alpha^{\text{KS}} = (\tau^{\text{KS}} - \tau^{\text{W}})/\tau^{\text{TF}}, \quad (18)$$

$$z(a, b) = 1 - \frac{\max(0, \tau(a, b) - \tau^{\text{W}})}{\tau(a, b)}, \quad (19)$$

$$\alpha(a, b) = \frac{\max(0, \tau(a, b) - \tau^{\text{W}})}{\tau^{\text{TF}}}. \quad (20)$$

The quantities z^{KS} and α^{KS} are the main τ^{KS} -dependent variables used in the construction of the meta-GGA exchange [9]. In Eqs. (19) and (20) they are regularized in order to satisfy the constraint of Eqs. (11) and (12). As previously mentioned, the regularization is very important near the core if $b \neq 0$; see also section Sec. IV A.

The indicators defined in Eqs. (14)-(16) express how much an approximated KED impacts on average on the accuracy of z^{KS} and α^{KS} as well as on a typical exchange

enhancement factor. Thus, they provide a measure on the expectable accuracy of each model for subsystem DFT calculations.

Finally, to obtain an overall assessment, we average, for each indicator, over M different systems as

$$\Delta_{\theta}(a, b) = \frac{1}{M} \sum_i^M \delta_{\theta}(a, b), \quad (21)$$

where $\theta = z, \alpha, \text{ or } x$.

III. COMPUTATIONAL DETAILS

A. Two-dimensional scan

To study the model of Eq. (13), we have performed a two dimensional scan over the parameters space $(a, b) \in [0, 2] \times [0, 4]$, considering the following training set: Ne₂, Ne-Ar, (CH₄)₂ (WI); (H₂S)₂, CH₃Cl-HCl, CH₃SH-HCN (DI); (HF)₂, (H₂O)₂, HF-HCN (HB); AlH-HCl, LiH-HCl, BeH₂-HF (DHB); NH₃-F₂, C₂H₂-ClF, H₂O-ClF (CT). For this set we have calculated the error indicators δ_z , δ_{α} , and δ_x defined by Eqs. (14)-(16). All quantities have been calculated on densities obtained from standard KS-DFT supermolecular calculations, using the PBE [74] XC functional. In some cases, approximate KED have been regularized imposing the constraint of Eq. (12), i.e. $\tau^{approx(reg.)} = \max(\tau^{approx}, \tau^W)$; see Eqs. (19), (20), and (31).

All molecular calculations have been performed using a locally modified version of the TURBOMOLE [75, 76] program package. In order to guarantee a good accuracy of the results and to minimize numerical errors, the supermolecular def2-TZVPPD [77, 78] basis set was employed in all calculations, together with very accurate integration grids (**grid 7, radsiz** 14). For all KS-DFT calculations tight convergence criteria were enforced, corresponding to maximum deviations in density matrix elements of 10^{-7} a.u.

For the noble atoms we used a fully numerical code [63] and the LDA functional.

B. Subsystem DFT

To assess the performance of the various τ models, we have employed them to carry on subsystem DFT calculations with meta-GGA XC functionals. In this case, we have computed the non-additive XC meta-GGA terms using the TPSS [8], revTPSS [10], BLOC [12, 13, 79], meta-VT{8,4} [80], and MGGA_MS2 [20] functionals. Note that the latter functional uses a GGA correlation expression, so the approximation concerns in this case only the exchange term. For all subsystem DFT calculations, we have considered a partition in two subsystems and we have performed a full relaxation of embedded ground-state electron densities through freeze-and-thaw

cycles [38, 43]. These calculations have been performed using the FDE script [56] of the TURBOMOLE program [75] considering as convergence criterion the difference of the dipole moments of the embedded subsystems ($< 10^{-3}$ a.u.). To compute the non-additive kinetic contributions [Eq. (6)] the revAPBEK kinetic functional [47, 48] has been employed. As to the non-additive meta-GGA XC term, we have employed the computational procedure described in Ref. 57 (i.e. substitution of τ^{KS} with a semilocal model) using the τ models described in Section II. Such calculations have been performed on the following sets of non-covalent complexes:

WI: weak interaction (He-Ne, He-Ar, Ne₂, Ne-Ar, CH₄-Ne, C₆H₆-Ne, (CH₄)₂)

DI: dipole-dipole interaction ((H₂S)₂, (HCl)₂, H₂S-HCl, CH₃Cl-HCl, CH₃SH-HCN, CH₃SH-HCl)

HB: hydrogen bond ((NH₃)₂, (HF)₂, (H₂O)₂, HF-HCN, (HCONH₂)₂, (HCOOH)₂)

DHB: double hydrogen bond (AlH-HCl, AlH-HF, LiH-HCl, LiH-HF, MgH₂-HCl, MgH₂-HF, BeH₂-HCl, BeH₂-HF)

CT: charge transfer (NF₃-HCN, C₂H₄-F₂, NF₃-HCN, C₂H₄-Cl₂, NH₃-F₂, NH₃-ClF, NF₃-HF, C₂H₂-ClF, HCN-ClF, NH₃-Cl₂, H₂O-ClF, NH₃-ClF).

The geometries as well as the reference binding energies were taken from Refs. 46, 81–84.

The accuracy of the subsystem DFT calculations has been measured considering the following two quantities. The first one is the error on the total embedding energy ΔE , defined as

$$\Delta E = E_{A+B}[\tilde{\rho}_A, \tilde{\rho}_B] - E^{\text{GKS}}[\rho^{\text{GKS}}], \quad (22)$$

where $E_{A+B}[\tilde{\rho}_A, \tilde{\rho}_B]$ is the total energy obtained from the subsystem DFT calculation, with $\tilde{\rho}_A$ and $\tilde{\rho}_B$ being the embedded subsystem densities and E^{GKS} being the conventional GKS total energy of the complex, computed at the “true” ground-state density ρ^{GKS} [48, 56, 85]. The second one is the embedding density error defined as

$$\xi = \frac{1000}{N} \int |\Delta\rho(\mathbf{r})| d\mathbf{r}, \quad (23)$$

where N is the total number of electrons and $\Delta\rho(\mathbf{r})$ is the deformation density

$$\Delta\rho(\mathbf{r}) = \tilde{\rho}_A(\mathbf{r}) + \tilde{\rho}_B(\mathbf{r}) - \rho^{\text{GKS}}(\mathbf{r}). \quad (24)$$

Note that only valence electron densities have been considered in the calculation of density errors [57].

Finally, to have an overall indication of the performance of the different τ approximations, we computed, within each group of molecules, the the mean absolute error (MAE) and the mean absolute relative error (MARE), the latter being referred to reference binding

energies [85]. Furthermore, we considered the two global quantities [48]

$$\text{rwMAE} = \frac{1}{5} \sum_i \left(\frac{MAE_i}{\langle MAE_i \rangle} \right) \quad (25)$$

$$\text{rwMARE} = \frac{1}{5} \sum_i \left(\frac{MARE_i}{\langle MARE_i \rangle} \right) \quad (26)$$

where the sums extend over WI, DI, HB, DHB, CT, and $\langle MAE_i \rangle$ ($\langle MARE_i \rangle$) is the average MAE (MARE) among the different methods considered for the class of systems i .

C. Embedding energy error decomposition

The error on embedding energy can be written [57, 85]

$$\Delta E = \Delta D + \Delta T_S + \Delta E_{xc} . \quad (27)$$

The error components are

$$\Delta D = E_H \left[\sum_I \rho_I \right] + \tilde{E}_{xc} \left[\sum_I \rho_I \right] + \left\{ E_H [\rho^{\text{GKS}}] + \tilde{E}_{xc} \left[\sum_I \rho^{\text{GKS}} \right] \right\} , \quad (28)$$

$$\Delta T_S = \tilde{T}_s^{\text{nadd}} - T_S[\Phi^{\text{GKS}}] - \sum_I T_s[\Phi^I] , \quad (29)$$

$$\Delta E_{xc} = \tilde{E}_{xc}[\rho^{\text{GKS}}] - \sum_I \tilde{E}_{xc}[\rho_I] - \left\{ E_{xc}[\Phi^{\text{GKS}}] - \sum_I E_{xc}[\Phi^I] \right\} , \quad (30)$$

where E_H is the Hartree energy (electron-electron and electron-nuclei classical Coulomb interaction energy), ρ^{GKS} and Φ^{GKS} are respectively the density and the Slater determinant of the supermolecular system as obtained from a standard GKS calculation, and the tilde ($\tilde{}$) denotes that an approximate functional form is considered.

IV. RESULTS

A. Two dimensional scan of the τ model

Figure 1 reports the values of the error indicators δ_z , δ_α , and δ_x [see Eqs. (14)-(16)] as computed for the Neon atom in the case of the KED model of Eq. (13). Similar results are found for Argon and Radon, see Fig. S1 of Ref. [86].

The most important result of Fig. 1 is that the minima for all the three indicators appear at $a = 0$ and $b \approx 2.2$: the latter almost coincide with the “non-empirical” value of $20/9$ (from the second-order gradient expansion).

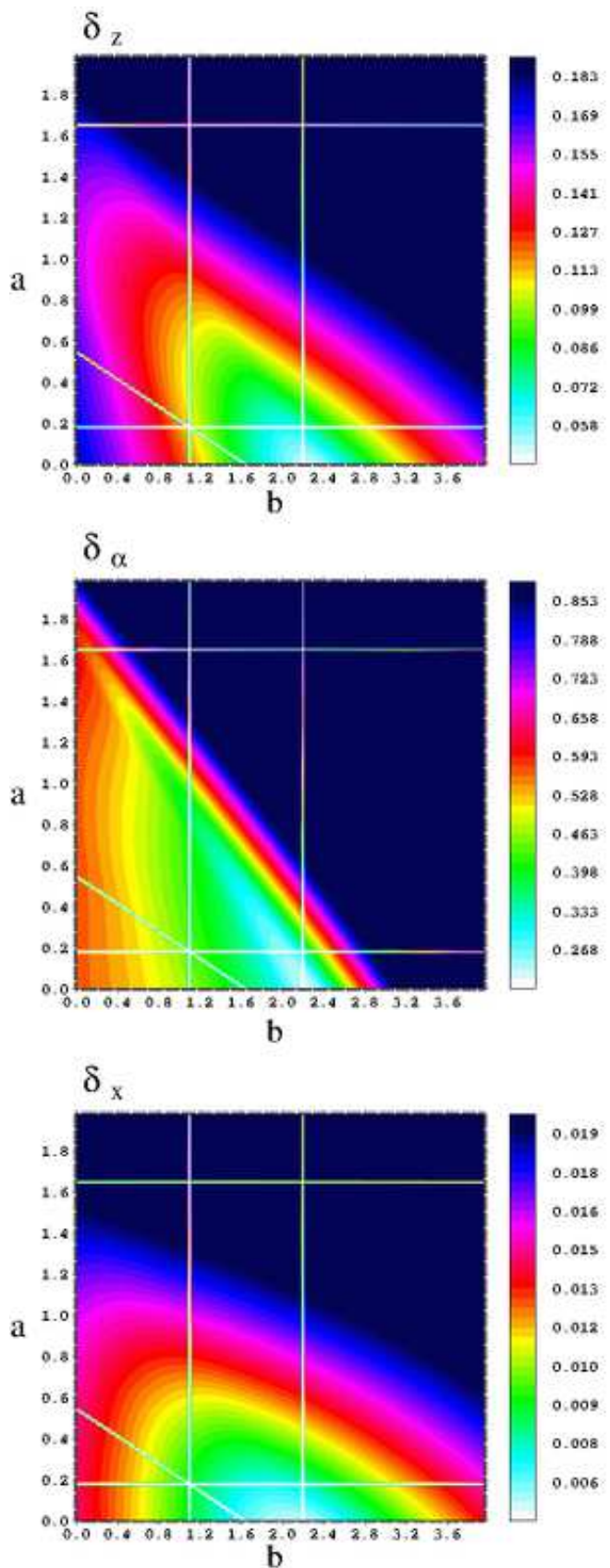


FIG. 1: Values of $\delta_z(a, b)$, $\delta_\alpha(a, b)$ and $\delta_x(a, b)$ [see Eqs. (14)-(16)] as functions of the values of the a and b parameters in Eq. (13) for the Neon atom. The white horizontal lines denote $a = 5/27$ and $a = 5/3$. The white vertical lines denote $b = 10/9$ and $b = 20/9$. The white diagonal line represents the Yang’s formula [Eq. (9)]. The color map is linear and, in each panel, it is limited to represent values not larger than four times the minimum value.

Similar findings have been obtained in Ref. [69], where the value of b had been fitted for different GGA KED, in order to reproduce the exact KED for the first 10 atoms (H-Ne) of the periodic table. The result in Fig. 1, is more general, because we demonstrate that $(a, b) = (0, 2.2)$ is the global minimum.

Thus we introduce a new KED model, named regularized Thomas-Fermi plus Laplacian (TFL), that is defined by the formulas

$$\tau^{TFL(reg.)} = \max(\tau^{TFL}, \tau^W), \quad (31)$$

$$\tau^{TFL} = \tau^{TF} \left(1 + \frac{20}{9}q \right). \quad (32)$$

We note again that the TFL model can be considered a “non-empirical” functional because it is defined with the coefficient $b = 20/9$ which comes from the second-order gradient expansion (however, it is not *ab initio*, because its general form is suggested by the numerical analysis of the error indicators). As the TFL model in Eq. (32) depends only on the Laplacian and not on the gradient, and it is not a LLMGGA kinetic energy functional. The TFL functional, instead, belongs to a different class of functionals which can be named Laplacian-Level density approximation (LLDA). On the other hand, its regularized version, i.e., the TFL(reg.) functional in Eq. (31), shall be considered as a conventional LLMGGA functional, as it also depends on the gradient of the density through τ^W . However, the regularization is only active near the core (see hereafter), which is not relevant for molecular applications. Thus, for simplicity, we will consider both TFL and TFL(reg.) as LLDA functionals, to distinguish them from other LLMGGA functionals which depend on the gradient also in the valence region.

Fig. 1 shows that the shapes of δ_z and δ_x are rather similar. This similarity is indeed not surprising because, as mentioned before, the z ingredient, tested in δ_z , is the main variable used to construct the meta-GGA TPSS exchange enhancement factor, which is used in the construction of δ_x . On the other hand, the δ_α plot looks quite different. Nevertheless, the minimum is still at $(a, b) \approx (0, 20/9)$.

Another interesting result of Fig. 1, is that TF, i.e. $(a, b) = (0, 0)$, and TFW, i.e. $(a, b) = (5/3, 0)$, yield almost the same values of δ_z and δ_α . This is due to error cancellation effects, as explained in Fig. 2, where the integrands of Eq. (14) and Eq. (15) are reported in the upper and lower panel, respectively.

Concerning the integrand of δ_z (upper panel), we see that TFW always underestimates the exact value, whereas TF(reg.) overestimates it, yielding similar global error δ_z . Concerning the integrand of δ_α (lower panel), one can see that TF(reg.) is better than TFW in the range to $r < 0.2$ a.u. and 0.5 a.u. $< r < 1.2$ a.u., whereas TFW is better than TF(reg.) in the range 0.2 a.u. $< r < 0.5$ a.u. and for $r > 1.2$ a.u., again yielding similar global error δ_α . Clearly, without regularization the results for TF will be much worse (see red dashed-lines in Fig. 2).

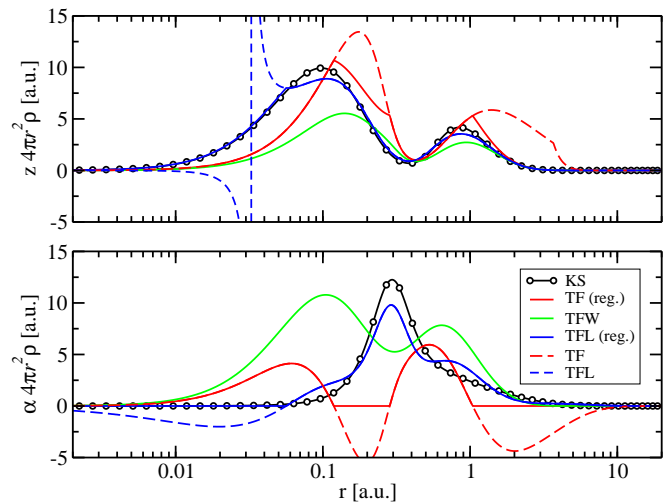


FIG. 2: Integrand of Eq. (14), upper panel, and Eq. (15), lower panel, versus the radial distance for the Neon atom for different KED models.

Figure 2 also shows the high accuracy of the TFL(reg.) model which matches the exact KS results everywhere in the space. Note that the regularization is very important when z^{KS} needs to be accurately reproduced near the core region, otherwise, as shown in the upper panel of Fig. 2, a divergence (i.e. at $r \approx 0.02$) will appear, as q becomes negative near the core. On the other hand, regularization is less critical for α^{KS} , as one can see comparing TFL and TFL(reg.) in the lower panel Fig. 2.

The above results are not limited to atoms, but hold also for molecules. Figure 3 reports a similar investigation as in Fig. 1 but averaged over a set of molecules (see Section III). Interestingly, the results for the three indicators are all similar to the ones shown in Fig. 1, with the minima again located at $(a, b) \approx (0, 20/9)$. This finding is quite important and confirms previous results for atoms.

Thus the TFL(reg.) model is the one that yields the best (average) performance among the models of the family defined by Eq. (13).

B. Comparison with other kinetic energy functionals

In Table I the performances of KED from different kinetic energy functionals are compared to TFL: we considered LDA, GGA and LLMGGA functionals. Note that all functionals are regularized, but TFW, mGGA and mGGArev which implicitly satisfy Eq. (12). The results in Tab. I show that TF and all GGAs give almost the same results for all indicators, as already discussed in section IV A.

Large improvements are only obtained when the Laplacian term is considered. The mGGA functional of Ref. [70] yields the best results for Δ_z and Δ_x , while TW02

TABLE I: Values of $\Delta_z(a, b)$, $\Delta_\alpha(a, b)$ and $\Delta_x(a, b)$ [see Eq.(21)] for different KED models evaluated on a molecular test set (see Section III for details). If applicable, also the values of the a and b parameters (as defined in Eq. (13)) and the literature reference are reported for each functional. The smallest values of the indicators for each class of functionals are highlighted in bold style.

Model	Reg.	Δ_z	Δ_α	Δ_x	a	b	Ref.
Local Density Approximation (LDA)							
TF	Yes	0.193	0.662	0.017	0	0	[61]
Generalized Gradient Approximation (GGA)							
TFW	Impl.	0.186	0.690	0.021	5/3	0	[57]
$\tau^{\text{TF}}(1 + \mu_{\text{GE2}}s^2)$	Yes	0.189	0.662	0.016	5/27	0	[65]
$\tau^{\text{TF}}(1 + \mu_{\text{MGE2}}s^2)$	Yes	0.188	0.662	0.017	0.2389	0	[68]
revAPBEK	Yes	0.188	0.662	0.017	-	0	[48]
TW02	Yes	0.189	0.663	0.017	-	0	[87]
LC94	Yes	0.189	0.663	0.017	-	0	[88]
Laplacian-Level Meta-GGA (LLMGGGA)							
GE2	Yes	0.068	0.281	0.007	5/27	20/9	[65]
MGE2	Yes	0.076	0.326	0.008	0.2389	20/9	[68]
τ^L	Yes	0.070	0.241	0.008	-	20/9	[57]
$\tau^{\text{TW02}} + \frac{20}{9}\tau^{\text{TF}}q$	Yes	0.068	0.233	0.007	-	20/9	[87]
$\tau^{\text{LC94}} + \frac{20}{9}\tau^{\text{TF}}q$	Yes	0.068	0.236	0.007	-	20/9	[88]
mGGA	Impl.	0.056	0.320	0.006	-	-	[70]
L0.4	Yes	0.189	0.663	0.017	-	-	[49]
L0.6	Yes	0.189	0.663	0.017	-	-	[49]
mGGArev	Impl.	0.096	0.323	0.010	-	-	[73]
Laplacian-Level Density Approximation (LLDA)							
TFL	Yes	0.050	0.203	0.005	0	20/9	this work

[87] regularized with $(20/9)q$, gives the best results for Δ_α ,

The last line of Tab. I shows that TFL model yields the best results overall, confirming the results of Sect. IV A.

C. Subsystem DFT calculations

In this section we apply the TFW, τ^L , and τ^{TFL} [Eq. (32)] KED models in subsystem DFT calculations using several different XC meta-GGA functionals. This can provide a practical assessment of the reliability of the different models. We consider TFW as a simple GGA satisfying Eq. (12), τ^L as a simple meta-GGA, previously considered in Ref. [57], and τ^{TFL} as the best functional, as discussed in the previous sections. Note that, in subsystem DFT, τ^L and τ^{TFL} can be also used *without regularization*. In fact, as discussed in Ref. [57], core contributions cancel out in the non-additive quantities.

In Fig. 4 we report (panel a) the rwMAE [Eq. (25)] for the embedding *densities* errors and (panel b) the rwMARE [Eq. (26)] for the embedding *energy* errors evaluated for all the investigated meta-GGA XC functionals and KED models. Results for all systems are reported in Ref. 86. Concerning the density error, we see that the

τ models containing the Laplacian term (i.e. τ^L and τ^{TFL}) perform very similarly and accurately, yielding rwMAE values in the range 0.90 – 0.98. The τ^{TFL} is better than τ^L only for the MS2 functional, while the performances are comparable for other meta-GGAs. On the other hand, the τ^{TFW} model displays a worse performance, providing rwMAE values oscillating between 1.06 – 1.13.

For the embedding energy error, the trend is the same as for the density errors: τ^L and τ^{TFL} provide the best performance with quite similar results, but for the BLOC functional where τ^{TFL} is distinctively better than τ^L . In all the cases the TFW model gives definitely poorer results yielding rwMARE values above 1.1 for all functionals (to be compared to values of about 0.9 for the τ^{TFL} and τ^L models) and it is very inaccurate for revTPSS and MS2.

For a deeper understanding of these results, it is possible to perform an embedding energy error decomposition analysis [57, 85] (see subsection III C for details). This allows to separate the relaxation error ΔD , due to the fact that the embedding density differs from the reference Kohn-Sham supermolecular one, from the errors arising from the approximations used in the non-additive energy functionals. The latter can be further divided into a kinetic energy error ΔT_S and an XC error ΔE_{xc} . The

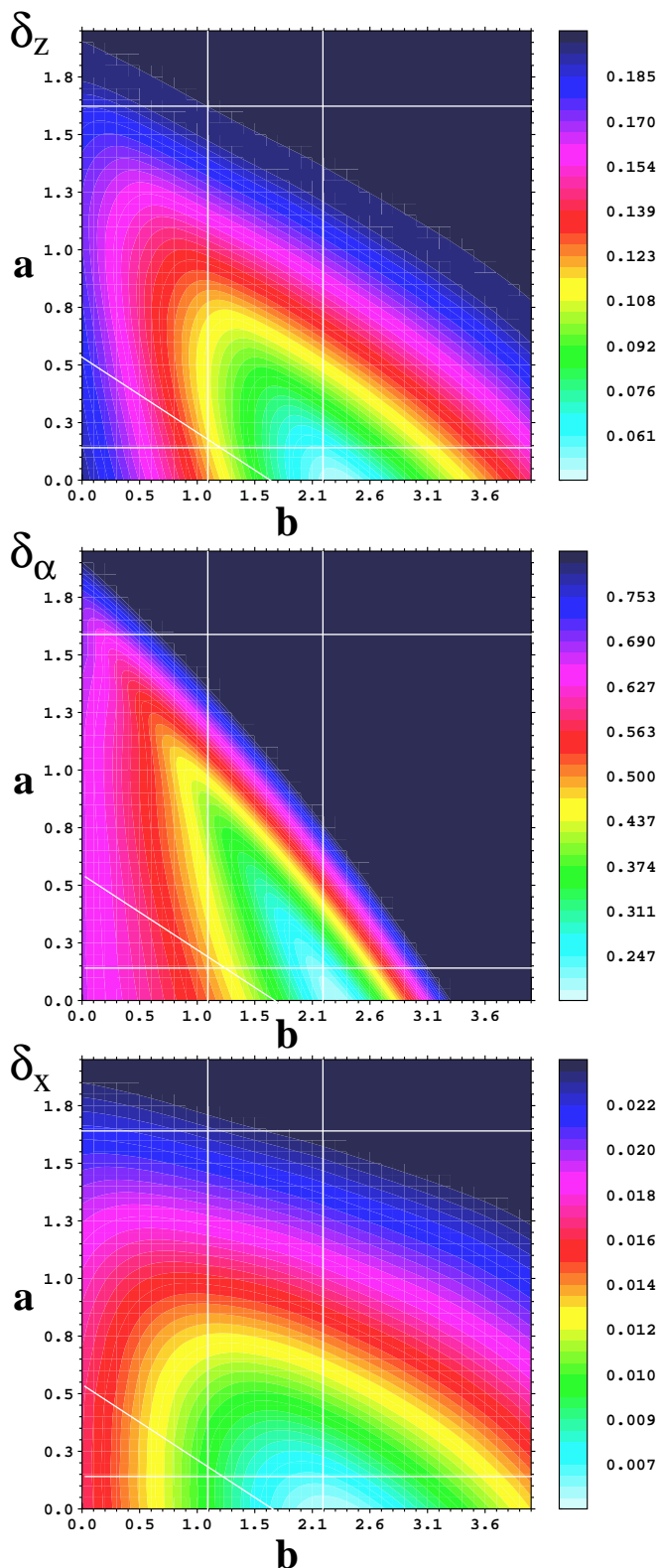


FIG. 3: Values of $\Delta_z(a, b)$, $\Delta_\alpha(a, b)$ and $\Delta_x(a, b)$ [see Eqs. 21]) as functions of the values of the a and b parameters in Eq. (13) for a set of molecules (see Sect. III). Other details are the same as in Fig. 1.

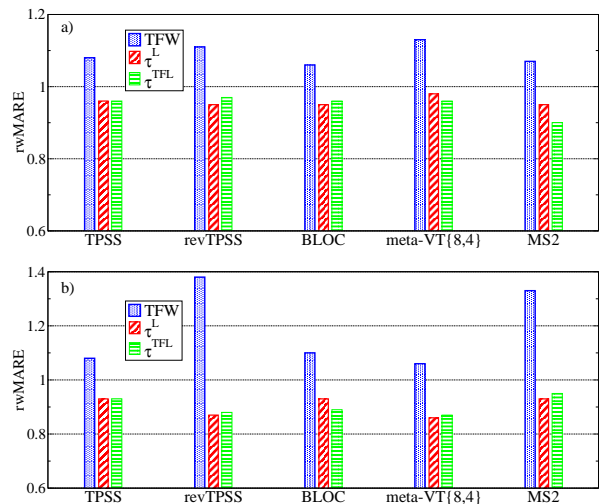


FIG. 4: Top: the rwMAE [Eq. (25)] for the embedding *densities* errors calculated for all the investigated meta-GGA XC functionals and τ models. Bottom: the rwMAE [Eq. (26)] for the embedding *energy* errors calculated for all the investigated meta-GGA XC functionals and τ models.

former originates from approximations used in Eq. (6) and, in the present calculations, it is the same for all cases (we used the revAPBEK kinetic functional in all calculations). The latter traces back to the use of a semilocal KED model to compute Eq. (7), for different meta-GGA XC functionals. Thus, this is the most interesting quantity in the present context.

Hence, we consider in Fig. 5 the average XC absolute ratio (AXCAR) [57] defined as

$$\text{AXCAR} = \frac{1}{M} \sum_{i=1}^M \frac{|\Delta E_{xc}|}{|\Delta E_{xc}| + |\Delta T_s + \Delta D|}, \quad (33)$$

where M is the number of systems in the test set (results for all systems are reported in supporting information). This provides an average absolute (i.e. without error compensation) measure of the XC contribution to the embedding energy error. Inspection of the figure shows that in all cases τ^L and τ^{TFL} yield AXCAR values much smaller than TFW (AXCAR always larger than 40%). Moreover, τ^{TFL} gives smaller AXCAR than τ^L , for all functionals, but revTPSS. These results indicate that the accuracy observed for the embedding energy error is not essentially due to some error compensation effect, but really traces back to a superior quality of the τ^{TFL} model in approximating the kinetic energy density contributions in the XC meta-GGA non-additive term.

V. SUMMARY AND CONCLUSIONS

In subsystem DFT the non-additive XC term must be an explicit functional of the density. Therefore, in order to be able to perform subsystem DFT calculations

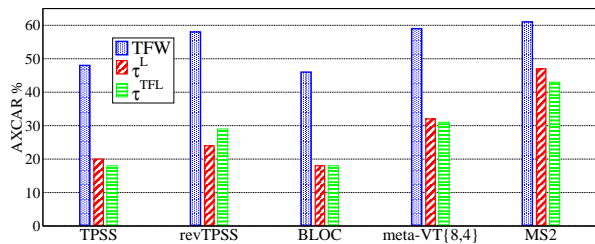


FIG. 5: The AXCAR error [Eq. (33)] calculated for different methods and τ models.

employing meta-GGA XC functionals, it is necessary to replace the positive-defined Kohn-Sham KED (τ^{KS}) with an approximated semilocal KED model (τ). The development of such a model is not as a hard task as the general development of accurate kinetic energy functionals because, in the context of subsystem DFT, only non-additive contributions are important. Thus, core contributions, which incorporate most of the Pauli kinetic energy, are not much relevant. On the other hand, in the present context, there is the need to model all the spatial features of the KED, since this is employed non-linearly inside meta-GGA XC functionals and not only to produce a kinetic energy (via integration) and/or a kinetic potential (via functional derivation). For this reason, for example, the accurate determination of the proper gauge for the KED is a crucial issue in this field. The development of accurate KED models is therefore a challenging and interesting topic that has practical relevance in subsystem DFT but is also of fundamental importance to understand the basic behavior of the kinetic energy, which is a key quantity in all areas of DFT.

In this work, we studied the problem of developing an accurate semilocal KED model by considering a flexible ansatz [Eq. (13)] depending linearly on the reduced gradient and Laplacian of the density. In this way, we found that a Laplacian contribution of the type $(1/6)\nabla^2\rho$ is essential to fix the correct gauge in the KED and thus to provide an accurate description of most of the features of the exact KDE. In fact, already a simple model (i.e. the TFL one of Eq. (31)) built from the Thomas-Fermi KED and the Laplacian correction (i.e. without any gradient correction), performs remarkably well for atoms and molecular complexes.

A thorough assessment work showed that the simple TFL model, is indeed able to capture most of the important features of the KED. Hence, in this context it outperforms all the known gradient expansion KED models (e.g. the conventional [64], modified [68], path-integral-derived [66] second-order gradient expansions) as well as many GGA and Laplacian-dependent meta-GGA models.

These findings are important for different topics in DFT. Clearly they are relevant for subsystem DFT calculations with meta-GGA XC functionals. Thus, they can allow to extend the applicability and accuracy of subsystem DFT, permitting to benefit from the advantages of meta-GGA XC functionals. Nevertheless, the general results of this work, concerning the role of dif-

ferent density contributions to the KED and especially that of the Laplacian, can have a larger impact on future work. They are in fact extremely relevant for all those studies and applications where a semilocal model of the KED is important. Here we suggest, for example, the evaluation of local indicators such as the electron localization function (ELF) [89, 90] or the entanglement length [91]. These are density indicators but they are actually obtained as orbital-dependent expressions due to the presence of τ^{KS} . The use of an appropriate semilocal KED model can turn them into true density indicators and largely extend their application domain providing as well a deeper understanding of the underlying physics and chemistry.

Acknowledgements

This work was partially supported by the National Science Center under Grant No. DEC-2013/11/B/ST4/00771.

Appendix A: Total energy and potential of the model KED of Eq. (8)

Consider the KED of Eq. (8). Note that it can be written

$$\tau = \tau^{\text{TF}} F(s) + \frac{3b}{10} \nabla^2 \rho = \tau^{\text{GGA}} + \frac{3b}{10} \nabla^2 \rho. \quad (\text{A1})$$

The corresponding total kinetic energy is

$$T_s = \int \tau^{\text{GGA}} d\mathbf{r} + \frac{3b}{10} \int \nabla^2 \rho d\mathbf{r} = T_s^{\text{GGA}} + \frac{3b}{10} \int \nabla^2 \rho d\mathbf{r}. \quad (\text{A2})$$

The last integral can be evaluated via the second Green's identity. Hence,

$$\int \nabla^2 \rho d\mathbf{r} = \int \nabla_{\perp} \rho dS + \int \rho \nabla^2 1 d\mathbf{r} = \int \nabla_{\perp} \rho dS, \quad (\text{A3})$$

where $\nabla_{\perp} \rho$ is the perpendicular component of the gradient with respect to the surface area element dS . For any finite system, with an exponentially decaying density, the integral in Eq. (A3) vanishes. Therefore, the Laplacian term does not contribute to the total kinetic energy.

Concerning the potential we have [9]

$$v_T = \frac{\partial \tau}{\partial \rho} - \nabla \cdot \frac{\partial \tau}{\partial \nabla \rho} + \nabla^2 \frac{\partial \tau}{\partial \nabla^2 \rho}. \quad (\text{A4})$$

For τ given by Eq. (8), that is

$$\begin{aligned} v_T &= \frac{\partial \tau^{\text{GGA}}}{\partial \rho} - \nabla \cdot \frac{\partial \tau^{\text{GGA}}}{\partial \nabla \rho} + \nabla^2 \frac{\partial (3b \nabla^2 \rho / 10)}{\partial \nabla^2 \rho} = (\text{A5}) \\ &= v_T^{\text{GGA}} + \frac{3b}{10} \nabla^2 \frac{\partial \nabla^2 \rho}{\partial \nabla^2 \rho} = v_T^{\text{GGA}} + \frac{3b}{10} \nabla^2 1 = v_T^{\text{GGA}}. \end{aligned}$$

-
- [1] W. Kohn and L. J. Sham, *Phys. Rev.* **140**, A1133 (1965).
- [2] J. F. Dobson, G. Vignale, and M. P. Das, *Electronic Density Functional Theory* (Springer, 1998).
- [3] G. E. Scuseria and V. N. Staroverov, in *Theory and Applications of Computational Chemistry: The First 40 Years (A Volume of Technical and Historical Perspectives)*, edited by C. E. Dykstra, G. Frenking, K. S. Kim, and G. E. Scuseria (Elsevier, Amsterdam, 2005), pp. 669–724.
- [4] J. P. Perdew and K. Schmidt, *AIP Conf. Proc.* **577**, 1 (2001).
- [5] D. C. Langreth and M. J. Mehl, *Phys. Rev. B* **28**, 1809 (1983).
- [6] J. P. Perdew, M. Ernzerhof, and K. Burke, *J. Chem. Phys.* **105**, 9982 (1996).
- [7] A. V. Arbuznikov, *J. Struct. Chem.* **48**, S1 (2007).
- [8] J. Tao, J. P. Perdew, V. N. Staroverov, and G. E. Scuseria, *Phys. Rev. Lett.* **91**, 146401 (2003).
- [9] F. Della Sala, E. Fabiano, and L. A. Constantin, *Int. J. Quantum Chem.* **116**, 1641 (2016).
- [10] J. P. Perdew, A. Ruzsinszky, G. I. Csonka, L. A. Constantin, and J. Sun, *Phys. Rev. Lett.* **103**, 026403 (2009).
- [11] L. A. Constantin, L. Chiodo, E. Fabiano, I. Bodrenko, and F. Della Sala, *Phys. Rev. B* **84**, 045126 (2011).
- [12] L. A. Constantin, E. Fabiano, and F. Della Sala, *Phys. Rev. B* **86**, 035130 (2012).
- [13] L. A. Constantin, E. Fabiano, and F. Della Sala, *Phys. Rev. B* **88**, 125112 (2013).
- [14] F. Della Sala, E. Fabiano, and L. A. Constantin, *Phys. Rev. B* **91**, 035126 (2015).
- [15] T. Van Voorhis and G. E. Scuseria, *J. Chem. Phys.* **109**, 400 (1998).
- [16] H. L. Schmider and A. D. Becke, *J. Chem. Phys.* **109**, 8188 (1998).
- [17] Y. Zhao and D. G. Truhlar, *J. Chem. Phys.* **125**, 194101 (2006).
- [18] A. Ruzsinszky, J. Sun, B. Xiao, and G. I. Csonka, *J. Chem. Theory. Comput.* **8**, 2078 (2012).
- [19] J. Sun, B. Xiao, and A. Ruzsinszky, *J. Chem. Phys.* **137**, 051101 (2012).
- [20] J. Sun, R. Haunschuld, B. Xiao, I. W. Bulik, G. E. Scuseria, and J. P. Perdew, *J. Chem. Phys.* **138**, 044113 (2013).
- [21] R. Peverati and D. G. Truhlar, *J. Phys. Chem. Letters* **3**, 117 (2012).
- [22] B. Xiao, J. Sun, A. Ruzsinszky, J. Feng, R. Haunschuld, G. E. Scuseria, and J. P. Perdew, *Phys. Rev. B* **88**, 184103 (2013).
- [23] J. Sun, B. Xiao, Y. Fang, R. Haunschuld, P. Hao, A. Ruzsinszky, G. I. Csonka, G. E. Scuseria, and J. P. Perdew, *Phys. Rev. Lett.* **111**, 106401 (2013).
- [24] V. N. Staroverov, G. E. Scuseria, J. Tao, and J. P. Perdew, *Phys. Rev. B* **69**, 075102 (2004).
- [25] C. Adamo, M. Ernzerhof, and G. E. Scuseria, *J. Chem. Phys.* **112**, 2643 (2000).
- [26] K. E. Riley, B. T. Op't Holt, and K. M. Merz, *J. Chem. Theory. Comput.* **3**, 407 (2007).
- [27] J. Sun, A. Ruzsinszky, and J. P. Perdew, *Phys. Rev. Lett.* **115**, 036402 (2015).
- [28] J. Sun, R. C. Remsing, Y. Zhang, Z. Sun, A. Ruzsinszky, H. Peng, Z. Yang, A. Paul, U. Waghmare, X. Wu, et al., *Nat. Chem.* **8**, 831 (2016), article.
- [29] H. S. Yu, X. He, and D. G. Truhlar, *J. Chem. Theory. Comput.* **12**, 1280 (2016).
- [30] J. Tao and Y. Mo, *Phys. Rev. Lett.* **117**, 073001 (2016).
- [31] J. Wellendorff, K. T. Lundgaard, K. W. Jacobsen, and T. Bligaard, *J. Chem. Phys.* **140**, 144107 (2014).
- [32] N. Mardirossian and M. Head-Gordon, *J. Chem. Phys.* **142**, 074111 (pages 1) (2015).
- [33] L. A. Constantin, E. Fabiano, J. Pitarke, and F. Della Sala, *Phys. Rev. B* **93**, 115127 (2016).
- [34] S. Kümmel and L. Kronik, *Rev. Mod. Phys.* **80**, 3 (2008).
- [35] A. V. Arbuznikov and M. Kaupp, *Chem. Phys. Lett.* **381**, 495 (2003).
- [36] F. Zahariev, S. S. Leang, and M. S. Gordon, *J. Chem. Phys.* **138**, 244108 (2013).
- [37] A. Seidl, A. Görling, P. Vogl, J. A. Majewski, and M. Levy, *Phys. Rev. B* **53**, 3764 (1996).
- [38] T. A. Wesolowski, in *Chemistry: Reviews of Current Trends*, edited by J. Leszczynski (World Scientific: Singapore, 2006, Singapore, 2006), vol. 10, pp. 1–82.
- [39] C. R. Jacob and J. Neugebauer, *Wiley Interdisciplinary Reviews: Computational Molecular Science* **4**, 325 (2014).
- [40] A. Krishtal, D. Sinha, A. Genova, and M. Pavanello, *J. Phys.-Condens. Mat.* **27**, 183202 (2015).
- [41] E. Prodan and W. Kohn, *PNAS* **102**, 11635 (2005).
- [42] T. A. Wesolowski and A. Warshel, *J. Phys. Chem.* **97**, 8050 (1993).
- [43] T. A. Wesolowski and J. Weber, *Chem. Phys. Lett.* **248**, 71 (1996).
- [44] A. W. Götz, S. M. Beyhan, and L. Visscher, *J. Chem. Theory Comput.* **5**, 3161 (2009).
- [45] T. A. Wesolowski, *J. Chem. Phys.* **106**, 8516 (1997).
- [46] T. A. Wesolowski, H. Chermette, and J. Weber, *J. Chem. Phys.* **105**, 9182 (1996).
- [47] L. A. Constantin, E. Fabiano, S. Laricchia, and F. Della Sala, *Phys. Rev. Lett.* **106**, 186406 (2011).
- [48] S. Laricchia, E. Fabiano, L. A. Constantin, and F. Della Sala, *J. Chem. Theory. Comput.* **7**, 2439 (2011).
- [49] S. Laricchia, L. A. Constantin, E. Fabiano, and F. Della Sala, *J. Chem. Theory. Comput.* **10**, 164 (2014).
- [50] F. Tran and T. A. Wesolowski, *Int. J. Quantum Chem.* **89**, 441 (2002).
- [51] F. Tran and T. A. Wesolowski, in *Recent Progress in Orbital-free Density Functional Theory*, edited by T. A. Wesolowski and Y. A. Wang (World Scientific, Singapore, 2013), pp. 429–442.
- [52] E. Fabiano, S. Laricchia, and F. Della Sala, *J. Chem. Phys.* **140**, 114101 (2014).
- [53] S. Laricchia, E. Fabiano, and F. Della Sala, *Chem. Phys. Lett.* **518**, 114 (2011).
- [54] T. A. Wesolowski, *Phys. Rev. A* **77**, 012504 (2008).
- [55] T. Dresselhaus and J. Neugebauer, *Theor. Chem. Acc.* **134**, 1 (2015).
- [56] S. Laricchia, E. Fabiano, and F. Della Sala, *J. Chem. Phys.* **133**, 164111 (2010).
- [57] S. Śmiga, E. Fabiano, S. Laricchia, L. A. Constantin, and F. Della Sala, *J. Chem. Phys.* **142**, 154121 (2015).
- [58] P. Ramos, M. Papadakis, and M. Pavanello, *J. Phys. Chem. B* **119**, 7541 (2015).
- [59] L. H. Thomas, *Proc. Cambridge Phil. Soc.* **23**, 542 (1926).

- [60] E. Fermi, *Rend. Accad. Naz. Lincei* **48**, 73 (1928).
- [61] E. Fermi, *Z. Phys.* **6**, 602 (1927).
- [62] C. F. von Weizsäcker, *Z. Phys. A* **96**, 431 (1935).
- [63] C. Ciraci and F. Della Sala, *Phys. Rev. B* **93**, 205405 (2016).
- [64] D. A. Kirzhnits, *Field theoretical methods in many-body systems* (Pergamon Press, 1967).
- [65] M. Brack, B. Jennings, and Y. Chu, *Phys. Lett. B* **65**, 1 (1976).
- [66] W. Yang, *Phys. Rev. A* **34**, 4575 (1986).
- [67] W. Yang, R. G. Parr, and C. Lee, *Phys. Rev. A* **34**, 4586 (1986).
- [68] D. Lee, L. A. Constantin, J. P. Perdew, and K. Burke, *J. Chem. Phys.* **130**, 034107 (2009).
- [69] D. Garcia-Aldea and J. E. Alvarelos, *J. Chem. Phys.* **127**, 144109 (2007).
- [70] J. P. Perdew and L. A. Constantin, *Phys. Rev. B* **75**, 155109 (2007).
- [71] V. V. Karasiev, R. S. Jones, S. B. Trickey, and F. E. Harris, *Phys. Rev. B* **80**, 245120 (2009).
- [72] V. V. Karasiev, D. Chakraborty, O. A. Shukruto, and S. B. Trickey, *Phys. Rev. B* **88**, 161108 (2013).
- [73] A. C. Cancio, D. Stewart, and A. Kuna, *J. Chem. Phys.* **144**, 084107 (2016).
- [74] J. P. Perdew, K. Burke, and M. Ernzerhof, *Phys. Rev. Lett.* **77**, 3865 (1996).
- [75] TURBOMOLE V6.2, 2009, a development of University of Karlsruhe and Forschungszentrum Karlsruhe GmbH, 1989-2007, TURBOMOLE GmbH, since 2007; available from <http://www.turbomole.com>.
- [76] F. Furche, R. Ahlrichs, C. Hättig, W. Klopper, M. Sierka, and F. Weigend, *Wiley Interdisciplinary Reviews: Computational Molecular Science* **4**, 91 (2014).
- [77] F. Weigend and R. Ahlrichs, *Phys. Chem. Chem. Phys.* **7**, 3297 (2005).
- [78] D. Rappoport and F. Furche, *J. Chem. Phys.* **133**, 134105 (2010).
- [79] L. A. Constantin, E. Fabiano, and F. Della Sala, *J. Chem. Theory. Comput.* **9**, 2256 (2013).
- [80] J. M. del Campo, J. L. Gázquez, S. Trickey, and A. Vela, *Chem. Phys. Lett.* **543**, 179 (2012).
- [81] Y. Zhao and D. G. Truhlar, *J. Phys. Chem. A* **109**, 5656 (2005).
- [82] Y. Zhao and D. G. Truhlar, *J. Chem. Theory and Comput.* **1**, 415 (2005).
- [83] S. Laricchia, E. Fabiano, and F. Della Sala, *J. Chem. Phys.* **138**, 124112 (2013).
- [84] E. Fabiano, L. A. Constantin, and F. Della Sala, *J. Chem. Theory. Comput.* **10**, 3151 (2014).
- [85] S. Laricchia, E. Fabiano, and F. Della Sala, *J. Chem. Phys.* **137**, 014102 (2012).
- [86] See supplementary material at <http://aip.scitation.org/doi/suppl/10.1063/1.4975092>.
- [87] F. Tran and T. A. Wesoloski, *Int. J. Quant. Chem.* **89**, 441 (2002).
- [88] A. Lembarki and H. Chermette, *Phys. Rev. A* **50**, 5328 (1994).
- [89] A. D. Becke and K. E. Edgecombe, *J. Chem. Phys.* **92**, 5397 (1990).
- [90] B. Silvi and A. Savin, *Nature* **371**, 683 (1994).
- [91] S. Pittalis, F. Troiani, C. A. Rozzi, and G. Vignale, *Phys. Rev. B* **91**, 075109 (2015).